

UNCLASSIFIED

Defense Technical Information Center  
Compilation Part Notice

ADP012574

TITLE: Comparative Experimental Study of Large-Scale Fluctuations in a Toroidally Magnetized Low-Beta Plasma

DISTRIBUTION: Approved for public release, distribution unlimited

This paper is part of the following report:

TITLE: Non-Neutral Plasma Physics 4. Workshop on Non-Neutral Plasmas [2001] Held in San Diego, California on 30 July-2 August 2001

To order the complete compilation report, use: ADA404831

The component part is provided here to allow users access to individually authored sections of proceedings, annals, symposia, etc. However, the component should be considered within the context of the overall compilation report and not as a stand-alone technical report.

The following component part numbers comprise the compilation report:

ADP012489 thru ADP012577

UNCLASSIFIED

# Comparative experimental study of large-scale fluctuations in a toroidally magnetized low- $\beta$ plasma

O. Grulke\*, F. Greiner<sup>†</sup>, T. Klinger\* and A. Piel<sup>†</sup>

\*MPI for Plasmaphysics, EURATOM Association, D-17491 Greifswald, Germany

<sup>†</sup>IEAP, Christian-Albrechts-University, D-24098 Kiel, Germany

**Abstract.** A comparative experimental study of large-scale space-time structures embedded into the broad-band multi-scale turbulent plasma fluctuations of the purely toroidally magnetized experiment TEDDI is presented. Two different plasma sources are compared: Plasma can be produced either by a thermionic discharge or by inductive heating by a helicon antenna. Turbulent plasma potential and plasma density fluctuations were analyzed by conditional averaging. It turned out that large-scale space-time structures develop on both plasmas, which propagate with local  $E \times B$  drift. A contribution of diamagnetic drifts is not observed. In the thermionic discharge dipole-like density structures are found, in the helicon discharge the detected structures are generally of monopole-like shape and are considerably sized when compared to the thermionic discharge. Direct measurements of the fluctuation induced transport can be related to the specific properties of the detected large-scale fluctuation structures. It is concluded that the injection of the negative space charge via the heated filament greatly alters the properties of the turbulent fluctuations. Although the basic statistical properties are substantially unaffected by the plasma source a strong influence on the formation of large-scale fluctuation structures and the associated transport is found.

## INTRODUCTION

It is a well known feature of turbulent systems that they develop large-scale space-time fluctuation structures. Fluctuation structures can be observed not only in plasmas but also in turbulence in neutral fluids, atmospheric turbulence etc. In plasmas the formation and properties of space-time fluctuation structures have been attracting great attention because they are suggested to contribute significantly to the fluctuation induced transport perpendicular to the magnetic field. The large fluctuation amplitudes can lead to large transport events and the large spatial extent of the structures leads to transport over large radial distances.

Experimentally, investigations of large-scale fluctuation structures were conducted in linear [1, 2, 3, 4] as well as in toroidal magnetic field geometry [5, 6, 7].

In linear geometry long-living large-scale monopole-like structures embedded into the turbulent plasma fluctuations were detected. In toroidal geometry large-scale fluctuation structures were also found but with different basic properties. Here, the detected structures have dipole-like shape. The interpretation of this difference is complicated because the effect of the magnetic field geometry in the toroidal devices are generally strongly entangled with effects arising from charge sources present to produce the plasma in

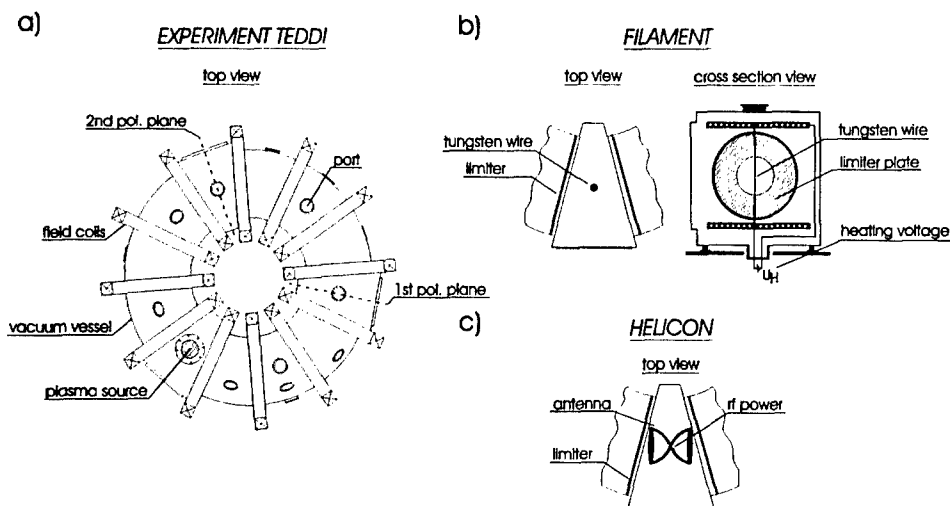


**FIGURE 1.** Schematic drawing of the TEDDI device (a) together with the two plasma sources, the filament source (b) and the helicon source (c).

these campaigns. Based on numerical simulations it was suggested that the formation of dipole-like structures can be mainly attributed to the presence of the charge source [8, 9]. To separate the geometry from plasma source effects an experimental study conducted in a device with simple toroidal magnetic field geometry is presented, in which two different plasma sources are used. First, plasma can be produced by the injection of highly energetic electrons, which is the standard method for plasma production in such devices. Alternatively, plasma can be produced 'quasineutral' by inductive heating without the injection of net charge.

This paper is organized as follows: After the introduction of the experimental setup the diagnostics and data analysis method of conditional averaging are briefly described. Subsequently the experimental results of conditional averaging for both plasmas and direct measurements of the fluctuation induced transport are presented. Finally, the results are summarized and conclusions are drawn.

## EXPERIMENTAL SETUP

The experiments were conducted in the toroidal plasma device TEDDI [10, 11, 12]. A schematic drawing of the device and the plasma sources is shown in Fig. 1. It consists of a toroidal vacuum chamber with three wedge-shaped segments, where the plasma

**TABLE 1.** Device and typical plasma parameters valid for the filament and helicon operation.

Parameter	Value
large device radius	0.3 m
small device radius	0.1 m
neutral Argon gas pressure	$3.2 \cdot 10^{-2}$ Pa
magnetic field	0.15 T
plasma density	$1 \cdot 10^{16}$ m <sup>-3</sup>
electron temperature	4 eV
ion temperature	0.03 eV
<u>filament operation:</u>	
discharge voltage	100 V
discharge current	0.2 A
<u>helicon operation:</u>	
rf frequency	28MHz
rf power	200W

source is placed and measurements of poloidal cross sections are performed. The device is magnetized by 12 planar poloidal magnetic field coils. Consequently, the magnetic field is purely toroidal. The typical magnetic field strength on the device axis is 0.15T. Plasma can be produced by two completely different discharge mechanisms: by direct injection of high energetic electrons (filament discharge) or by inductive coupling (helicon discharge). For the filament discharge (Fig. 1(b)) a tungsten wire is inserted into the vacuum vessel. The wire is directly heated by a DC current and the emitted electrons are accelerated between the negatively biased filament and the grounded poloidal limiters placed on both sides of the source region. Plasma is produced by ionizing collisions between the primary electrons and the Argon neutral gas background.

Alternatively, the plasma can be produced inductively. For this discharge mode a helicon antenna [13] (double-half-turn right-helical antenna) is installed at the position of the filament (Fig. 1(c)). Measurements of the magnetic wave field suggest that a helicon  $m = 1$  mode is driven by the antenna at a rf-frequency of 10-30MHz [10]. With a rf-power of 200W similar plasma density and electron temperature are obtained when compared to the filament discharge.<sup>1</sup> The basic device and plasma parameters are compiled in Tab. 1. The important difference between the two discharge types is that a strong negative source of charge is present in the filament generated plasma whereas plasma production is 'quasineutral' in the helicon discharge. This difference facilitates for direct investigation of the influence of net sources of charge on the formation and properties of large-scale fluctuation structures.

<sup>1</sup> It should be noted that helicon discharge in this context does not indicate the very efficient antenna-plasma coupling that leads to 100% ionization degree [14]

## DIAGNOSTICS AND DATA ANALYSIS

Measurements are performed with electric probes exclusively. Equilibrium plasma parameter profiles are obtained by evaluation of Langmuir probe characteristics. For density fluctuation measurements Langmuir probes are negatively biased and the ion saturation current fluctuations are taken as proportional to density fluctuations. For plasma potential fluctuations emissive probes are used, which are fairly insensitive against hot electron components [15, 16]. Fluctuation induced transport measurements are performed with triple probes.

Large-scale fluctuation structures are extracted out of the noise-like turbulent fluctuations by the statistical method of conditional averaging (CA). In its simplest form CA is based on two simultaneously recorded time series: On fluctuation time series  $\Phi_{\text{ref}}$  is recorded at a fixed spatial point  $\vec{r}_0$  and acts as the reference signal for the analysis. Another fluctuation time series  $\Phi_{\text{pos}}$  is recorded at an arbitrary second spatial position  $\vec{r}_0 + \Delta\vec{r}$ , here called the positioned signal. By a predefined condition  $\rho$  on  $\Phi_{\text{ref}}$  characteristic events in the time series are detected. Together with a time interval  $\Delta\tau$  around these time instants  $t_i$  an ensemble of sub-time series out of  $\Phi_{\text{mov}}$  of length  $N$  are collected, which are taken as statistical independent realizations of a random process. Consequently, ensemble averaging of the sub-time series extracts the part of fluctuations, which is consistently repeated in the sub-time series (coherent part) whereas the incoherent fluctuations are suppressed. The procedure reads:

$$\Phi_{\text{con}}(\vec{r}_0 + \Delta\vec{r}, \tau) = \frac{1}{N} \sum_{i=1}^N [\Phi_{\text{pos}}(\vec{r}_0 + \Delta\vec{r}, t_i + \tau) | \Phi_{\text{ref}}(\vec{r}_0, t_i) = \rho] . \quad (1)$$

The idea of conditional average is as follows: If a large-scale fluctuation structure passes the position of the reference probe, it produces a specific signal pattern in  $\Phi_{\text{ref}}$ , which is detected by the condition  $\rho$ . If the structure, depending on its lifetime and propagation, reaches the positioned probe, a similar signal pattern is produced in  $\Phi_{\text{pos}}$ . By taking the time instants  $t_i$  as the reference time for the analysis, the phase relation of structures occurring in the reference and positioned signal is conserved and ensemble averaging extracts the structure from the superimposed random turbulent background fluctuations. To obtain a confidence level for CA a conditional deviation is defined as the standard deviation at each time lag  $\tau \in \Delta\tau$  of the difference between the conditionally averaged structure and the single realization of the sub-time series. This quantity is normalized to the standard deviation of the reference signal

$$\sigma_{\text{CA}}(\vec{r}_0, \tau) = \frac{\sigma([\Phi_{\text{con}}(\vec{r}_0, \tau) - \Phi_{\text{ref}}(\vec{r}_0, t_i + \tau)]_{i=1 \dots N})}{\sigma(\Phi(\vec{r}_0, t))} . \quad (2)$$

A value of  $\sigma_{\text{CA}}$  well below unity indicates that the single realizations are reproducible whereas values close to one indicates that the single realizations strongly deviate from the average result.

For the current analysis an amplitude condition of  $1\sigma$  together with a rising slope condition is used. The slope condition ensures that events are always found on the same slope of the fluctuation signal and artificial phase shifts due to the finite widths of the fluctuations are avoided.

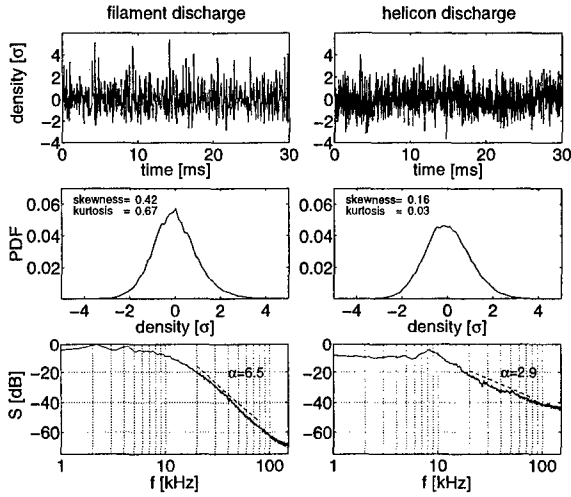


**FIGURE 2.** Density fluctuations (top row) with the respective probability distribution function (middle row) and power spectral densities (bottom row) for the filament (left column) and the helicon discharge (right column)

## EXPERIMENTAL RESULTS

### *Basic statistical properties of turbulent fluctuations*

In Fig. 2 time series of plasma density fluctuations are shown for both discharges together with their probability distribution function (PDF) and their power spectral density. The density fluctuations in both discharges show an irregular behavior. In the filament discharge fluctuations are slightly burst-like, whereas in the helicon discharge the density fluctuations show a noisy behavior. This is also expressed by the PDF, which is peaked and asymmetric for the filament discharge. This is quantified by the non-zero higher moments skewness and kurtosis (note that a Gaussian distribution has  $s=0$ ,  $k=0$  in this representation). In the helicon discharge the PDF is of almost perfect Gaussian shape. Both power spectral densities show a power law decrease  $S(f) \propto f^{-\alpha}$  over one frequency decade, which indicates that both plasmas are in a fully developed turbulent state [17]. The decrease is stronger in the filament plasma with a spectral index of  $\alpha = 6.5$  whereas in the helicon plasma the spectral index is  $\alpha = 2.9$ .

### *Conditional averaging results*

In Fig. 3 typical results of CA of the reference and positioned probe are presented for both discharge types. The reference signals show a pronounced positive fluctuation structure, which is mainly induced by the positive amplitude condition met at  $\tau = 0$ . The temporal width of the pattern is larger for the filament plasma when compared to the

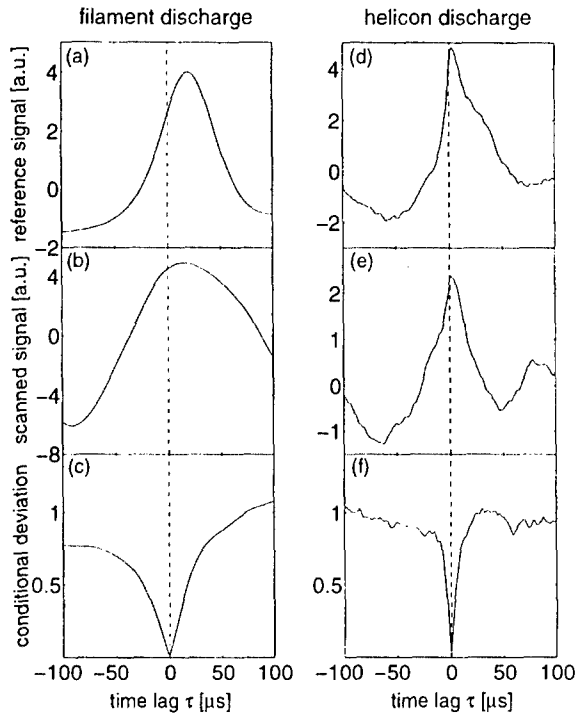


**FIGURE 3.** Conditional averaging signal at a single spatial point. Shown are the conditionally averaged reference signals (a), (d), the conditionally averaged positioned signals (b), (e), and the respective conditional deviations as defined in Eq. 2 (c), (f) for the filament and the helicon discharge

helicon plasma. Stronger differences are found in the positioned signal. Here, a dipole-like behavior is observed in the filament plasma with negative and positive amplitudes of similar magnitude. In the helicon plasma the conditionally averaged positioned signal shows a positive amplitude fluctuation with only little adjacent minima. The conditional deviation is zero at the time instant where the condition is fulfilled and increases with increasing absolute value of the time lag  $\tau$ . It is noticeable that the temporal confidence interval is larger in the filament plasma than in the helicon plasma.

To obtain space-time information of large-scale fluctuation structures measurements of density fluctuations are performed in a two-dimensional section perpendicular to the magnetic field lines. The results are shown in Fig. 4 for the filament generated plasma and in Fig. 5 for the helicon plasma.

*Filament discharge.* In Fig. 4 the results of CA of density fluctuations for a complete poloidal section are shown in normalized values. The time interval extends over  $160\mu\text{s}$ . The cross at  $\tau = 0$  indicates the position of the reference probe. Large-scale minimum fluctuation structures with adjacent maximum structures are found in the complete time window under consideration. Thus, the observed structure always appear in a dipole-like configuration. The minimum structure propagates radially outwards during the first

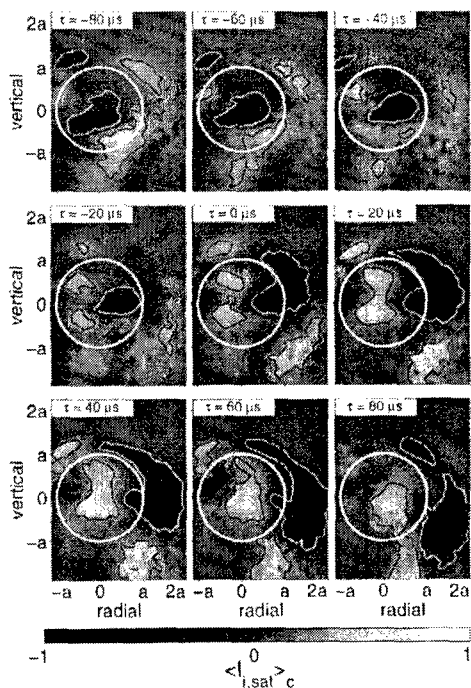


**FIGURE 4.** Conditional averaging results in a two-dimensional plane for density fluctuations in the filament discharge. The ambient magnetic field points into the plane. The solid white circle indicates the inner limiter radius. Minimum and maximum structures are emphasized by white and black contour lines, respectively, which represent a level of 30% of the peak amplitudes. The labeling of the radial and vertical axes are in units of the inner limiter radius  $a$ .

half of the time window  $\tau = -80 \dots 0 \mu s$  and poloidally during the second half from  $\tau = 0 \dots 80 \mu s$ . The same propagation properties are found for the maximum structure. Comparison of the propagation properties with the equilibrium potential profile yields that the propagation of the structures is fully determined by background  $E \times B$  drift, which is well distinguishable from diamagnetic drifts due to the strongly asymmetric plasma potential and plasma pressure profiles [10, 12]. The lifetimes of the detected structures are larger than the chosen time interval and the spatial extent are of the order of the plasma radius.

*Helicon discharge.* A different picture is obtained in the helicon discharge. The results of conditional averaging are shown in Fig. 5 in the same representation as Fig. 4. Here a negative density fluctuation structure develops at  $\tau = 0 \dots 80 \mu s$ , propagates radially towards the device center and decays at  $\tau = -20 \mu s$ . At the same time a maximum structure rapidly grows at  $\tau = -20 \dots 0 \mu s$ , is turned at the center of the device and decays at  $\tau = 40 \dots 60 \mu s$ . It is visible that both structures do not exist simultaneously. Thus, the structure are of monopole-like shape. The lifetime is significantly reduced and the structures are sized when compared to the structures found in the filament plasma.

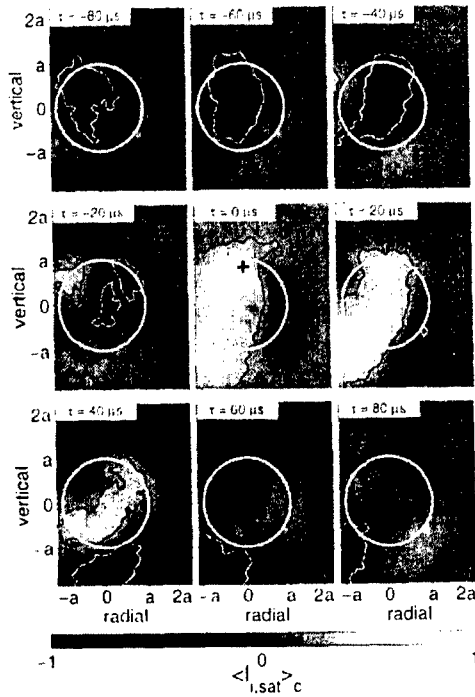


**FIGURE 5.** Conditional averaging results of density fluctuations for the helicon plasma in the same representation as Fig. 4

### *Fluctuation induced transport*

An important parameter for the fluctuation induced transport associated with space-time fluctuation structures is the phase relation between plasma potential and plasma density fluctuations. To obtain the phase information for the large-scale fluctuation structures under investigation the CA procedure was repeated in the two-dimensional spatial domain with plasma potential fluctuations as reference signal. Similar structures were found as shown in Figs. 4 and 5, but phase shifted by  $\approx \pi/2$ , which results in a strong fluctuation induced transport caused by the structures [12]. Fig. 6 shows the two-dimensional amplitude coherence between plasma potential and plasma density fluctuations, the directly measured fluctuating transport at the plasma outside, and its probability distribution function. The amplitude coherence show a broad structure, which strongly suggests, that the formation of structures is based on a MHD instability [18]. This is consistent with the observed large phase shift between plasma density and plasma potential fluctuations. The fluctuating transport and their respective PDF's for the filament and helicon plasma show significant differences. In the filament generated plasma the transport is burst-like with large transport events directed outwards. The PDF is peaked and asymmetric towards large transport events. In the helicon plasma a more noise-like transport is observed with a symmetric PDF. This can be directly related to

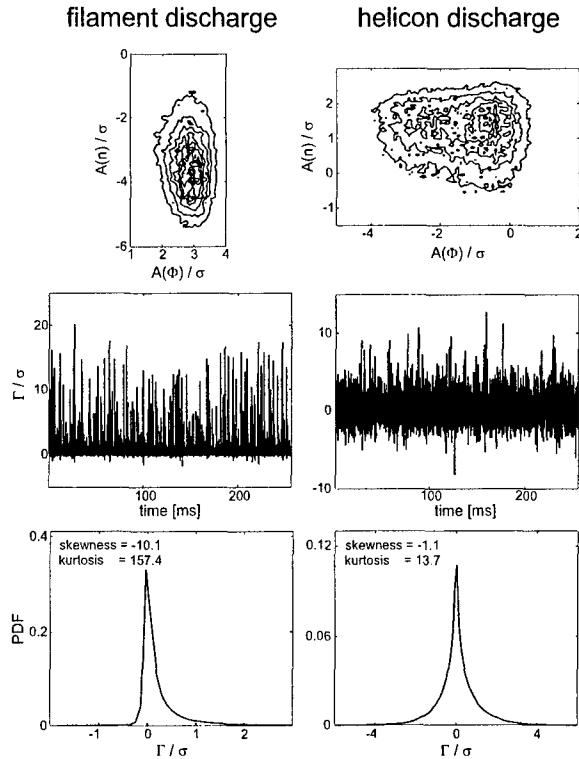


**FIGURE 6.** Two-dimensional amplitude probability distribution function between plasma density and plasma potential fluctuations (top row), time series of the measured fluctuation induced transport (middle row) and the respective PDF (bottom row).

the dynamical properties of the observed large-scale structures. In the filament plasma the spatial region of existence of structures is mainly outside and the phase relation between density and potential structures lead to a transport caused by these structures that is directed outwards. This strongly suggests that the large transport events are associated with these structures. In the helicon plasma structures exist in the plasma center and the phase shift between plasma density and plasma potential fluctuations is such that the resulting transport is directed towards the device center [12]. Consequently, no exposed large transport events are found and the PDF is symmetric.

## CONCLUSIONS

The presented experimental study was addressed to the question, what determines the specific properties of large scale turbulent fluctuation structures. By operating the device with two completely different plasma sources geometry effects could be separated from source-induced effects. Large-scale structures were found in both plasmas, which

propagate with local background  $E \times B$  drift. In contrast to linear magnetic field geometry, where generally small phase shifts between large-scale plasma potential and plasma density fluctuations are observed, the magnetic curvature in toroidal magnetic field geometry leads for both plasma sources to a large phase shift of  $\pi/2$ . This is consistent with numerical simulations, which includes both, curvature driven instabilities and drift waves, and measurements of the amplitude coherence between plasma density and plasma potential fluctuations. But the plasma source has a great influence on the specific shape and lifetime of structures. If negative space charge is injected into the plasma by the filament, structures generally appear dipole-like and have long lifetime. In the helicon discharge, where plasma is produced quasineutral, the structures are of monopole-like shape and their lifetime is considerably reduced when compared to the filament generated plasma. Specific features of the measured fluctuation induced transport can be attributed to the large-scale structures. In the filament plasma the propagation and phase shift of structures lead to transport events that dominate the transport time series. In the helicon plasma no significant contribution to the transport radially outwards due to the detected structures is expected and consistently the measured transport is more noise-like.

The results indicate that it is not sufficient to include only the magnetic geometry in the interpretation of particular properties of turbulent plasma fluctuations. As it was explicitly demonstrated for large-scale fluctuation structures, the plasma source can strongly alter the turbulent fluctuations and the associated transport.

## REFERENCES

1. Huld, T., Nielsen, A. H., Pécseli, H. L., and Rasmussen, J. J., *Phys. Fluids B*, **3**, 1609–1625 (1991).
2. Pécseli, H. L., Coutusias, E. A., Huld, T., Lynov, J. P., Nielsen, A. H., and Rasmussen, J. J., *Plasma Phys. Controlled Fusion*, **34**, 2065–2070 (1992).
3. Nielsen, A. H., Pécseli, H. L., and Rasmussen, J. J., *Physica Scripta*, **51**, 633–637 (1995).
4. Grulke, O., Klinger, T., and Piel, A., *Phys. Plasmas*, **6**, 788–796 (1999).
5. Endler, M., Giannone, L., Holzhauser, E., Niedermeyer, H., Rudyj, A., Theimer, G., Tsois, N., and ASDEX Team, *Nucl. Fusion*, **35**, 1307–1339 (1995).
6. Øynes, F. J., Pécseli, H. L., and Rypdal, K., *Phys. Rev. Lett.*, **75**, 81–84 (1995).
7. Joseph, B. K., Jha, R., Kaw, P. K., Mattoo, S. K., Rao, C. V. S., Saxena, Y. C., and the ADITYA team, *Phys. Plasmas*, **4**, 4292–4300 (1997).
8. Rypdal, K., Fredriksen, H., Paulsen, J. V., and Olsen, O. M., *Physica Scripta*, **T63**, 167–173 (1996).
9. Rypdal, K., Garcia, O. E., and Paulsen, J.-V., *Phys. Rev. Lett.*, **79**, 1857–1860 (1997).
10. Greiner, F., Grulke, O., Lechte, C., and Piel, A., “RF-plasma in a simple magnetized torus”, in *Proc. 2000 Int. Congress on Plasma Physics*, Quebec City, Canada, 2000, vol. 1, pp. 140–143.
11. Grulke, O., Greiner, F., Klinger, T., and Piel, A., “Spatiotemporal analysis of electrostatic fluctuations in a simple magnetized torus”, in *Proc. 2000 Int. Congress on Plasma Physics*, Quebec City, Canada, 2000, vol. 1, pp. 284–287.
12. Grulke, O., Greiner, F., Klinger, T., and Piel, A., *Plasma Phys. Controlled Fusion*, **43**, 525–542 (2001).
13. Light, M., and Chen, F. F., *Phys. Plasmas*, **2**, 1084–1093 (1995).
14. Chen, F. F., *Phys. Plasmas*, **3**, 1783–1793 (1996).
15. Wang, E. Y., Hershkowitz, N., Intrator, T., and Forest, C., *Rev. Sci. Instrum.*, **57**, 2425–2431 (1986).
16. Hershkowitz, N., and Cho, M. H., *J. Vac. Sci. Technol. A*, **6**, 2054–2059 (1988).
17. Frisch, U., *Turbulence: The Legacy of A. N. Kolmogorov*, Cambridge University Press, 1995.
18. Scott, B., *Phys. Plasmas*, **7**, 1845–1856 (2000).